

## Characterization of Natural Rubber/Gold Nanoparticles SERS-Active Substrate

Flávio C. Cabrera,<sup>1</sup> Deuber L. S. Agostini,<sup>1</sup> Renivaldo J. dos Santos,<sup>1</sup> Silvio R. Teixeira,<sup>1</sup> Miguel A. Rodríguez-Pérez,<sup>2</sup> Aldo E. Job<sup>1</sup>

<sup>1</sup>Faculdade de Ciências e Tecnologia, UNESP, Departamento de Física, Química e Biologia, CP 467, CEP 19060-080, Presidente Prudente, SP, Brasil

<sup>2</sup>CellMat laboratory, Condensed Matter Physics Department, University of Valladolid, 47011 Valladolid, Spain

Correspondence to: A. E. Job (E-mail: job@fct.unesp.br)

**ABSTRACT:** Natural rubber/gold nanoparticles membranes (NR/Au) were studied by ultrasensitive detection and chemical analysis through surface-enhanced Raman scattering and surface-enhanced resonance Raman scattering in our previous work (Cabrera et al., J. Raman Spectrosc. 2012, 43, 474). This article describes the studies of thermal stability and mechanical properties of SERS-active substrate sensors. The composites were prepared using NR membranes obtained by casting the latex solution as an active support (reducing/establishing agents) for the incorporation of colloidal gold nanoparticles (AuNPs). The nanoparticles were synthesized by *in situ* reduction at different times. The characterization of these sensors was carried out by thermogravimetry, differential scanning calorimetry, scanning electron microscopy (SEM) microscopy, and tensile tests. It is suggested an influence of nanoparticles reduction time on the thermal degradation of NR. There is an increase in thermal stability without changing the chemical properties of the polymer. For the mechanical properties, the tensile rupture was enhanced with the increase in the amount of nanoparticles incorporated in the material. © 2013 Wiley Periodicals, Inc. J. Appl. Polym. Sci. 000: 000–000, 2013

**KEYWORDS:** biomaterials; elastomers; properties and characterization; mechanical properties; nanoparticles; nanowires and nanocrystals

Received 3 October 2012; accepted 8 February 2012; published online

DOI: 10.1002/app.39153

### INTRODUCTION

Looking for renewable raw materials of low cost that meet the requirements of the consumer market, many countries consider the natural rubber (NR) as a profitable and safe alternative investment. Currently, the global production of latex concentrate in three regions, Asia 93.3%, Africa 4.5%, and Latin America 2.2%.<sup>1,2</sup>

Among the 2.2% of latex produced in Latin America, 54% is related to Brazil supply, which represents 1.2% of the world production.<sup>3,4</sup> This latex is mainly obtained from *Hevea brasiliensis* trees, originated in regions of humid, tropical climate, and temperatures ranging 25°C. Thus, it generates not only jobs and raw material production but an important support for environmental protection, since for each ton of NR produced, 4.8 tons of carbon from the synthetic rubber production are not emitted. It fits the culture of withdrawal and avoided emission of carbon,<sup>5</sup> targets established by the Kyoto Protocol and pled by several countries around the world.

Moreover, studies about the latex constituent<sup>6–8</sup> show that it is a colloidal system (rubber particles suspended in aqueous medium) called serum (dispersive medium), and known as a polymer of high molecular weight whose structure is *cis*-1,4-polyisoprene. The natural latex is composed of three phases that are obtained by centrifugation: rubber, serum, and bottom fraction. The rubber phase consists of 96% of hydrocarbon, 1% of protein, and 3% of lipids and traces of magnesium, potassium, and copper. The serum phase, also known as serum C or aqueous phase, presents different types of compounds, including carbohydrates, proteins, amino acids, enzymes, and nitrogenous bases.

Previous studies reported the use of latex for the synthesis of silver nanoparticles.<sup>9–12</sup> In addition, silver and gold nanostructures of different sizes, shapes, and with variable degree of plasmon coupling are mainly used for surface-enhanced Raman scattering (SERS) and surface-enhanced resonance Raman scattering (SERRS) substrates.<sup>13–16</sup>

Additional Supporting Information may be found in the online version of this article.

© 2013 Wiley Periodicals, Inc.

In other words, NR is a promising substrate with application in biological and medical fields because it can allow the stimulation of angiogenesis in the tissue.<sup>17–20</sup> The medical-pharmacological field has also led to a detailed study of parameters, such as pH, ionic strength, and kinetics growth, with the control of the structures at molecular levels. Thus, systems have been developed to incorporate drugs of interest, especially phospholipids films to simulate biological systems through the use of different polymeric materials.<sup>21–23</sup> Natural polymers, such as chitosan, fulvic acid, and starch, have also been explored in recent years for the synthesis of metal nanoparticles,<sup>24–26</sup> based on green chemistry as an advantageous and simple synthetic route.

The synthesis of gold nanoparticles (AuNPs) with NR films is simpler than making an Au colloid and casting it onto a substrate surface or preparing an Au evaporated film. Moreover, the cost of NR/Au substrate is low when compared to usual SERS substrates. Studies about the influence of NR/Au composite in *Leishmania* promastigotes growth was also carried out as an application for the material.<sup>27</sup>

In this study, a detailed characterization of both thermal and mechanical properties of the NR/Au composites via thermogravimetry (TG), differential scanning calorimetry (DSC), and stress–strain tests is reported.

## EXPERIMENTAL

NR membranes were prepared using latex from *H. brasiliensis* trees (RRIM 600) from the city of Indiana, São Paulo State, Brazil. The samples were collected from different trees. The membranes were prepared by casting method and were annealed at 65°C for 10 h in an oven. The latex was stabilized in ammonium hydroxide (2% vol). The dry rubber content of the latex was around 40 wt % and membranes were obtained with 0.5 mm of thickness.

The synthesis of the AuNPs was carried out by *in situ* reaction using gold chloride (AuCl<sub>3</sub>) 99.99% (Aldrich, Saint Louis, USA) in aqueous solution of  $3.1 \times 10^{-4}$  M, according to the methods described for colloids preparation by chemical reduction.<sup>28</sup> The reduction times were 6, 9, 15, 30, and 60 min of immersion of the NR membranes into the AuCl<sub>3</sub> aqueous solution at 80°C. Due to the fact that the membrane contains reducing agents, such as organic acids, it is not necessary to use citrate, hydroxylamine, or other reducing agents.<sup>27,29</sup>

### Characterization

SEM measurements were carried out using a FEI Quanta 200 FEG microscope with Field Emission Gun (filament), equipped with an Everhart-Thornley Secondary Electron Detector, and a Solid State Backscatter Detector with acceleration voltage of 15 kV and pressure of 1.00 Torr approx. (Low Vacuum), at CellMat laboratory of the Condensed Matter Physics Department in University of Valladolid. The tests of DSC were performed on a Netzsch model 214 Phoenix. About 5.0 mg of the samples were deposited on aluminum pans with a heating rate of 10°C/min. The temperature range used was from –120 to 500°C in N<sub>2</sub> atmosphere with a flow of 15 mL/min. TG analysis were carried out in a Netzsch model 209. About 15.0 mg of the samples were deposited in an alumina crucible, and pure nitrogen gas (N<sub>2</sub>) as the carrier gas

(15 mL/min). The heating rate was 10°C/min and the temperature range between 25 and 600°C. Both TG and DSC tests were performed using STDQ600 (TA Instruments) in oxidizing atmosphere (air), at a temperature range starting from room temperature to 1200°C. The heating rate was 10°C/min, the mass samples approximately 15.0 mg and carrier gas flow of 100 mL/min. The strain–stress test was performed by stretching the sample in EMIC model DL2000, at 500 mm/min and using an intern deformation transducer. The sample preparation was carried out according to ASTM D412 type C.

## RESULTS AND DISCUSSION

The synthesis of AuNPs was studied by SEM microscope. It was observed that with the increase of the reduction time, there was an increase in the amount and size of nanoparticles deposited on the NR surface, as presented in Figure 1(a–e) and Supporting Information Figure S1(a–e). The nanoparticles size was around 34 nm for NR/Au 6 min. This size increases to 47 nm for the NR/Au 30 min. The distribution showed a relative homogeneity of size and shape. Most particles are spherical; however, aggregates of smaller particles (NR/Au 9 min) were found on the surface of the NR, as shown in Figure 1(b). In addition, some areas on the surface contain high density of nanoparticles, Supporting Information Figure S1(c,d). The NR membranes, with 60 min of reduction, presented the formation of AuNPs out of the plane of the membranes surface. The coalescence of the nanoparticles can be observed after this time.

The spherical structure of AuNPs was reported in previous studies.<sup>29</sup> It was observed that the nanoparticles diffuse around 2 μm into the NR bulk.

Energy dispersive X-ray (EDX) spectroscopy coupled to SEM microscope was used to analyze the structural properties of the AuNPs on the most aggregated region of the membrane, NR/Au 30 min (Figure 2). Results showed that the nanoparticles are effectively gold (Au).<sup>30,31</sup> The oxygen and carbon compounds are attributed to the NR membrane that supports the nanoparticles.

Thermal analyses were carried out in an inert (nitrogen (N<sub>2</sub>)) and oxidant (Air) atmosphere. The DSC results, in N<sub>2</sub>, for the samples of NR and the composites obtained at 6, 9, 15, 30, and 60 min of reduction times, are shown in Figure 3. It is observed an endothermic event around –67°C, characteristic of glass transition temperature ( $T_g$ ). An endothermic depression around 100°C is attributed to the water present in the sample. The two exothermic peaks observed at 390 and 510°C correspond to the beginning and end of the structural degradation process of the polymer, respectively.<sup>32</sup>

The glass transition ( $T_g$ ) and degradation temperatures of the NR, for pure NR and NR/Au membranes, are shown in Table I. For different reduction times, the glass transition temperature and thermal degradation remained unchanged. The flexible properties of NR are attributed to low interchain crosslinking and the rotation of C–C bonds of monomers linkage. In the temperature of glass transition, the rubber loses the flexibility and changes to a brittle state. Therefore, the glass transition is attributed to the monomer unit of *cis*-1,4-polyisoprene. This

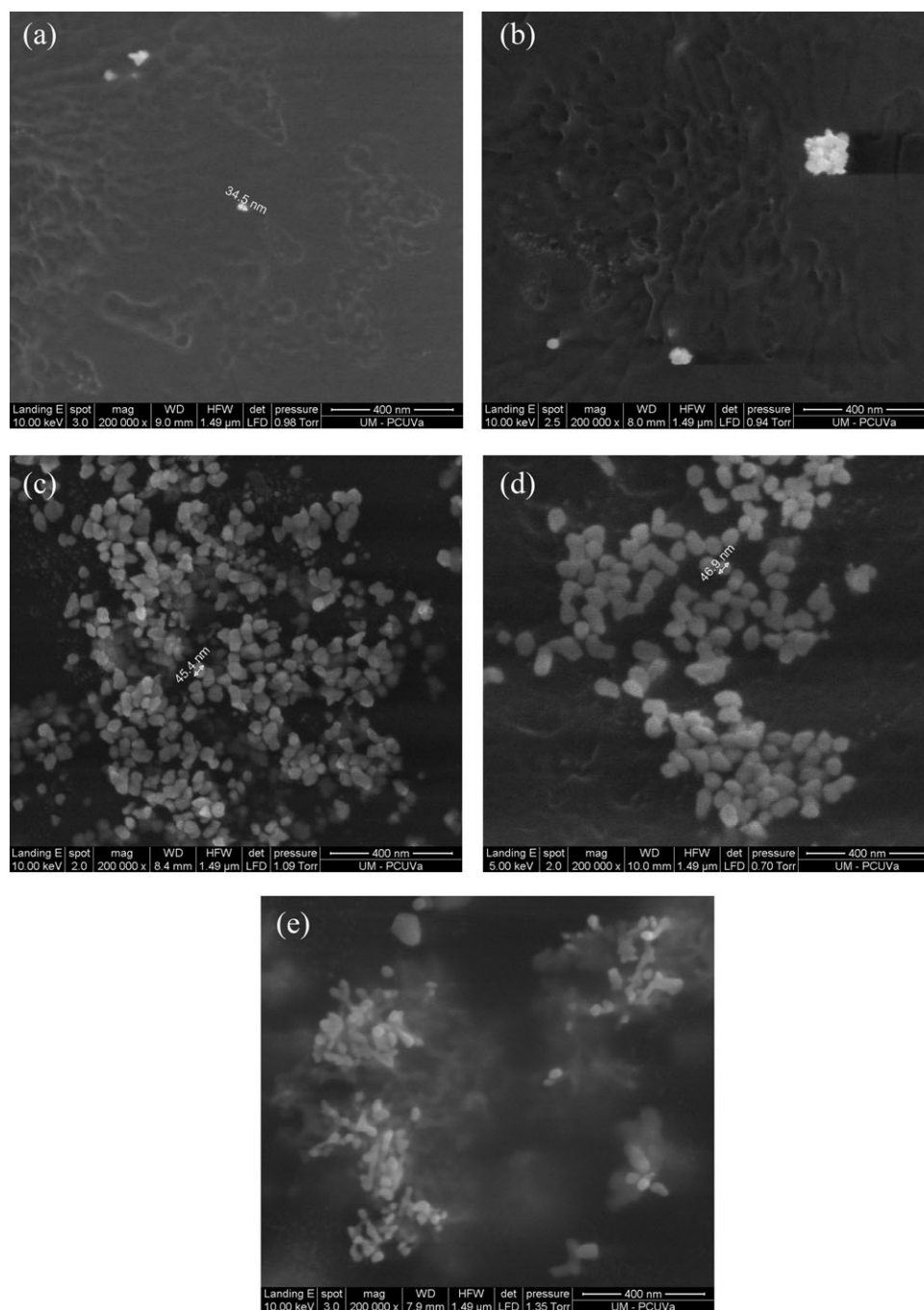


**Figure 1.** SEM images of NR/Au membranes in different reduction time (a) 6; (b) 9; (c) 15; (d) 30, and (e) 60 min. The NR/Au membranes were synthesized at 80°C in AuCl<sub>3</sub> aqueous solution ( $3.1 \times 10^{-4}M$ ).

result demonstrates that the incorporation of AuNPs did not influence in the main polymer structure.

The DSC analysis carried out in oxidizing atmosphere, Figure 4, exhibits different results when compared to those obtained in inert atmosphere. The formation of a shoulder between 222 and 310°C can be due to the initial degradation of the membranes and the peak between 327 and 348°C does not present similar characteristics to assume a structural modification. However, it

can be related to the degradation of the compounds used as precursors for the synthesis of the nanoparticles. They are released in the solution by NR membranes and adsorbed on the surface of the membranes with nanoparticles, as it becomes more evident after 30 min of reduction. The first stage of thermal decomposition of isoprene chains is between 367 and 381°C and the peak with maximum temperature between 497 and 507°C is attributed to the second stage of the polymeric chain thermal degradation.<sup>7,32</sup>

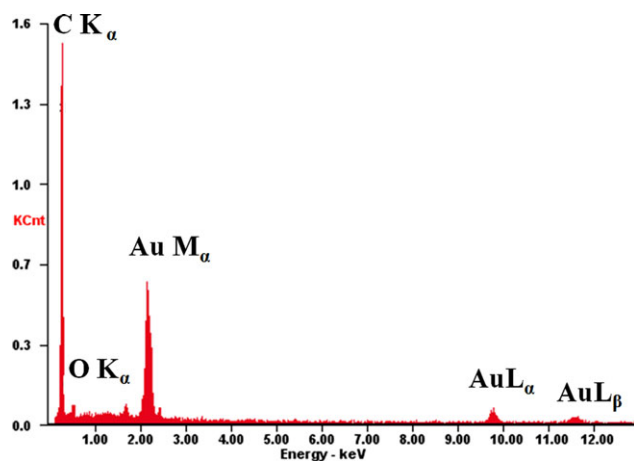


**Figure 2.** EDX/SEM results of NR with AuNPs at 30 min of reduction, synthesized at 80°C in AuCl<sub>3</sub> aqueous solution ( $3.1 \times 10^{-4}M$ ). [Color figure can be viewed in the online issue, which is available at [wileyonlinelibrary.com](http://wileyonlinelibrary.com).]

Comparing the DSC analysis in N<sub>2</sub> and air atmosphere, it is observed the occurrence of anticipated and more evident thermal reactions due to the oxidation effect that influences the membranes degradation. The change in relation to the baseline of NR/Au membranes, around 1060°C, is attributed to the melting point of AuNPs embedded in the polymer matrix.

The DSC analysis (Table I) shows an increase in the intensities of the peaks with the increase of the reduction time. This may be related to the release of compounds, such as aromatic organic acids or amides, responsible for the reduction of NR membranes, so that the interaction of the nanoparticles intensifies the reactions. However, this interaction is not sufficient to change the glass transition temperature of the membranes as the interaction does not occur in the main bonds of isoprene.

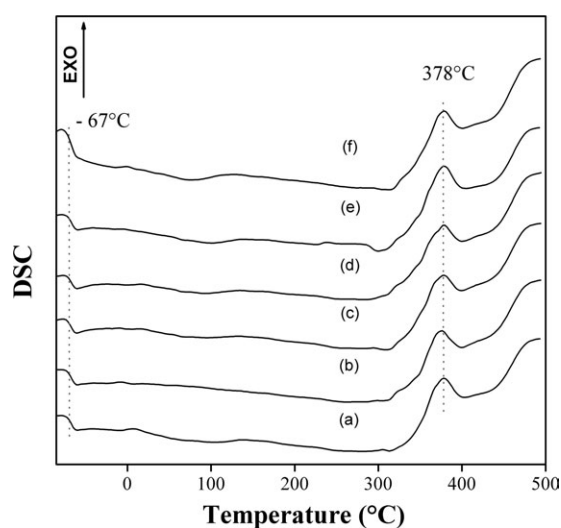


**Figure 3.** DSC analysis (N<sub>2</sub> atmosphere) of the membranes: (a) pure NR; NR/Au (b) 6 min; (c) 9 min; (d) 15 min; (e) 30 min; and (f) 60 min reduction time. The tests were carried out with 5.0 mg of each sample.

**Table I.** Comparison of Thermal Degradation Temperatures Obtained by DSC Technique for Both Pure NR and NR/Au Membranes (Air Atmosphere), and Comparison of Glass Transition Temperature and Thermal Degradation of Both Pure NR and NR/Au Membranes (N<sub>2</sub> Atmosphere)

Samples	DSC (N <sub>2</sub> )		DSC (O <sub>2</sub> )		
	T <sub>g</sub> (°C)	Thermal degradation (°C)	Temperature range (°C)	Temperature maximum (°C)	Heat flow (mW)
NR	-66.8	378.2	220-410	374.4	147.5
NR/Au 6 min	-66.2	379.3	410-559	483.5	152.3
			412-557	497.3	169.5
NR/Au 9 min	-67.0	378.1	226-400	370.7	170.5
			400-557	505.1	170.4
NR/Au 15 min	-66.5	378.5	210-403	373.9	180.2
			403-557	506.3	176.2
NR/Au 30 min	-66.4	378.4	216-404	368.4	189.1
			404-556	506.6	180.1
NR/Au 60 min	-66.9	378.8	214-408	375.7	196.3
			408-562	506.5	203.1

Thermogravimetric analysis (Figure 5) and first derivative thermogravimetric (DTG) curves (Supporting Information Figure S2) for NR and NR/Au membranes show a mass loss of 5% between 100 and 250°C, attributed to the release of water molecules and processes of crosslinking and scission of the polymeric chains. The crosslinking is associated to the formation of

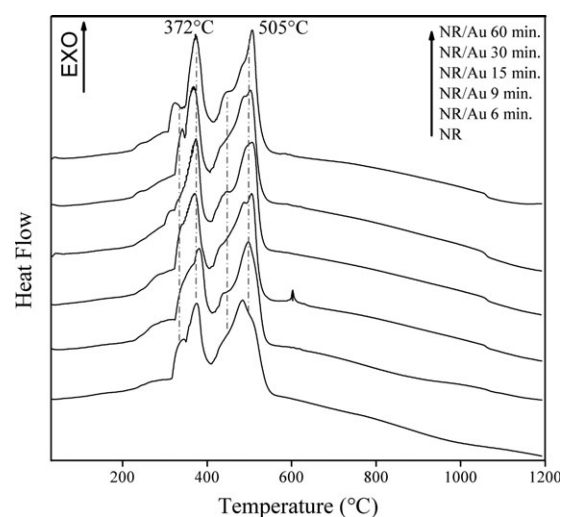


**Figure 4.** DSC Analysis (air atmosphere) of both NR and NR/Au membranes at different reduction time. The tests were carried out with 15.0 mg of each sample.

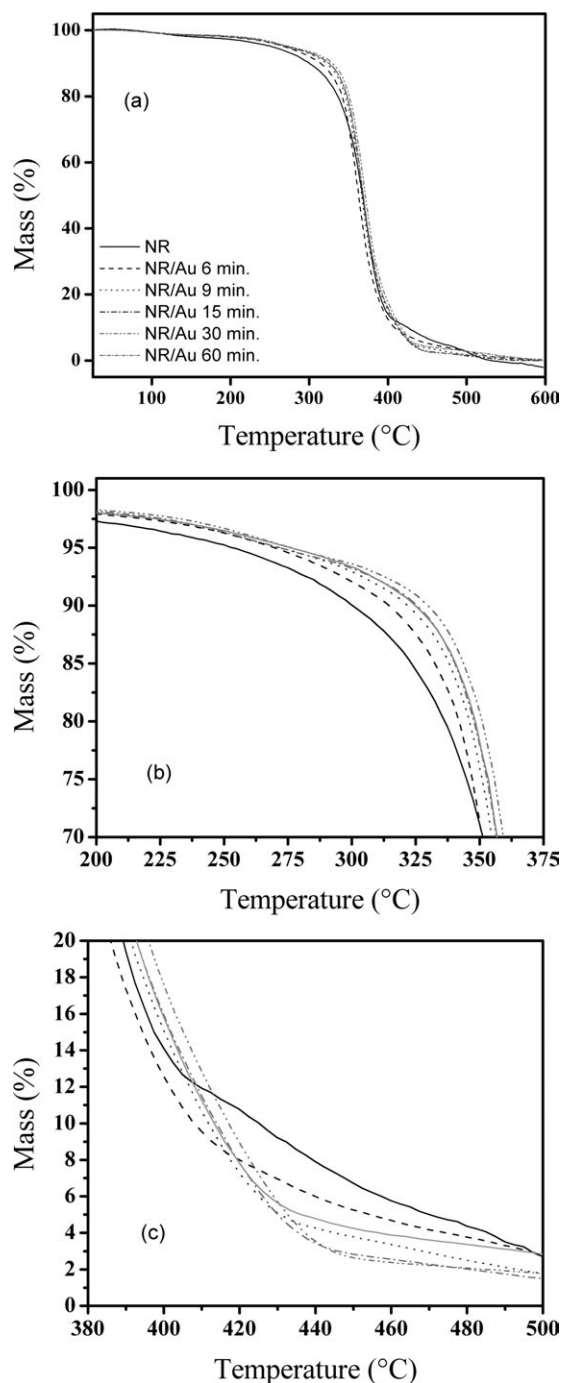


**Figure 5.** (a) TG analysis of both NR and NR/Au membranes at different reduction times. Emphasis of (b) first step of degradation, (c) second step of degradation ( $N_2$  atmosphere).

aldehydes, ketones, and carboxylic acids. In the zoom of the second degradation stage [Figure 5(b)], there is an increase in thermal stability until the reduction time of 30 min. This stability decreases for NR/Au 60 min samples, probably reaching a plateau. It can be due to an interaction between the components released into the solution of NR membranes and the samples which are now covered with metal nanoparticles. It avoids the

**Table II.** Comparison of Thermal Degradation Temperatures Obtained by Analysis of TG Technique for Both Pure NR and NR/Au Membranes ( $N_2$  and Air atmosphere)

Samples	Degradation temperature ( $N_2$ )			Degradation temperature ( $O_2$ )	
	Begin of degradation (On Set)	Temperature maximum ( $^{\circ}C$ )	NR (wt %)	End step of degradation (On Set)	End two steps degradation ( $^{\circ}C$ )
NR	340.1	373.6	83.71	403.1	495.4
NR/Au 6 min	342.9	363.3	85.27	407.0	495.5
NR/Au 9 min	345.3	364.4	83.08	427.7	508.0
NR/Au 15 min	346.1	369.2	83.80	431.5	492.7
NR/Au 30 min	349.1	370.4	84.0	437.5	486.6
NR/Au 60 min	347.3	368.7	83.32	424.9	490.5



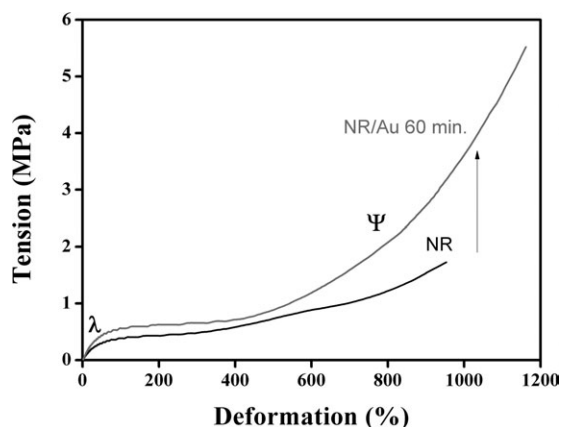


**Figure 6.** Stress–strain tests of both NR and NR/Au membranes at different reduction times. The sample was prepared according to ASTM D412 type C.

direct reaction between the polymer and nanoparticles in solution, in other words, after this time a new layer formation of nanoparticles occurs on the first layer. The degradation process which starts around 250°C and ends around 400°C, observed in the thermogram, shows a mass loss of 83–85%, characteristic of isoprene and subproducts degradation such as amides, amines, proteins, carbohydrates, among others.

The DTG curve (Supporting Information Figure S2) presented a shoulder around 400°C and can be attributed to a slower degradation of the polymer chains or highly crosslinked polymeric residues, which supports the idea of an increase of the composites thermal stability with the incorporation of AuNPs [Figure 5(c)].<sup>7,8,33</sup> Depressions are still observed at 425 and 510°C in the DTG curve of pure NR membrane. This process is related to the degradation of more stable latex products, which decreases with the incorporation of nanoparticles. The thermogravimetric analysis in oxidizing atmosphere (Table II) shows that the reactions occur at lower temperatures when compared to the analysis in inert atmosphere due to the interaction with oxygen.<sup>7,34</sup>

Figure 6 presents the mechanical properties by stress–strain tests of NR and NR/Au. It was observed a similar behavior for all samples. Firstly, it was identified an elastic deformation ( $\lambda$ ) and then a plastic deformation ( $\Psi$ ).<sup>35</sup> There was an increase in the tensile rupture when compared to the pure NR, which is proportional to the increase of the reduction time (Table III). On

**Table III.** Results From Stress–Strain Tests Evaluating Both NR and NR/Au Membranes at Different Reduction Times

Sample	Rupture deformation (%)	Tension (MPa)
NR	922 ± 59	1.95 ± 0.39
NR/Au 6 min	1191 ± 69	4.78 ± 0.31
NR/Au 9 min	1169 ± 139	4.74 ± 0.58
NR/Au 15 min	1185 ± 80	5.01 ± 0.25
NR/Au 30 min	1152 ± 111	5.10 ± 0.21
NR/Au 60 min	1126 ± 68	6.22 ± 0.90

the other hand, it is seen a nonlinear enhancement of the deformation of the NR/Au composites. Therefore, it can be affirmed that there is a mechanical reinforcement (filler agent) that enhances the tensile strength of composites due to the size and distribution of AuNPs on NR membranes.

## CONCLUSION

The formation of AuNPs on NR membranes by deposition kinetics has been studied. It was observed that the metal incorporation does not influence the polymer structure attributed to the DSC analysis that presented little variations in the glass transition temperatures when compared to the results obtained for pure NR membrane. For TG analysis, there is an increase in thermal stability with the increase of the reduction time when nanoparticles are incorporated. The strain–stress tests showed that the presence of nanoparticles in NR membranes allows a mechanical reinforcement (filler agent) which improves the tensile strength of the composites.

## ACKNOWLEDGMENTS

The authors acknowledge Fundação de Amparo a Pesquisa do Estado de São Paulo (FAPESP), the Instituto Nacional de Eletrônica Orgânica (INEO), NanoBioNet and NanoBioMed groups for financial support.

## REFERENCES

- International Rubber Study Group (IRSG). Rubber Industry Report; Singapore, **2009**, Vol. 8, No. 7–9. Available at: <http://www.docstoc.com/docs/22680242/International-Rubber-Study-Group-RUBBER-INDUSTRY-REPORT>
- ANRPC. Monthly Bulletin of Rubber Statistics; The Association of Natural Rubber Producing Countries (ANRPC); Malaysia, **2009**, Vol. 1, No. 1.
- Dall’Antonia, A. C.; Martins, M. A.; Moreno, R. M. B.; Mattoso, L. H. C.; Job, A. E.; Ferreira, F. C.; Gonçalves, P. S. *Polímeros* **2006**, 16, 239.
- Martins, M. A.; Forato, L. A.; Colnago, L. A.; Job, A. E.; Moreno, R. M. B.; Mattoso, L. H. C.; Gonçalves, P. S. In 8th Congresso Brasileiro de Polímeros, Águas de Lindóia, SP, Brazil, **2005**.
- Fernandes, T. J. G. Congresso brasileiro de heveicultura; Departamento de Ciências Agrárias Universidade Federal do Acre (UFAC): Vitória, ES; **2007**.
- Ferreira, M.; Moreno, R. M. B.; Gonçalves, P. S.; Mattoso, L. H. C. *Boletim de Pesquisa Embrapa*; São Carlos - SP, Brazil, **1999**, ISSN 1517–476X. Available at: [http://www.cnpdia.embrapa.br/publicacoes/download.php?file=BP08\\_99.pdf](http://www.cnpdia.embrapa.br/publicacoes/download.php?file=BP08_99.pdf)
- Rippel, M. M. Ph.D. Thesis, Caracterização Microestrutural de filmes e partículas de látex de borracha natural; Universidade Estadual de Campinas UNICAMP: Instituto de Química; **2005**.
- Agostini, D. L. S.; Dissertation Master’s Degree, Caracterização dos constituintes do látex e da borracha natural que estimulam a angiogênese, V. 87, A221c, Faculdade de

- Ciências e Tecnologia - FCT/UNESP, Presidente Prudente, SP, Brazil, 2009.
9. Bar, H.; Bhui, D. Kr.; Sahoo, G. P.; Sarkar, P.; De Sankar, P.; Misra, A. *Colloids Surf. A* **2009**, 339, 134.
  10. Abu Bakar, N. H. H.; Ismail, J.; Bakar, M. A. *Mater. Chem. Phys.* **2007**, 104, 276.
  11. Abu Bakari, M.; Ismail, J.; Teoh, C. H. *J. Rubber Res.* **2008**, 11, 196.
  12. Abu Bakar, M.; Ismail, J.; Teoh, C. H.; Tan, W. L.; Abu Bakar, N.N.H. *J. Nanomater.* **2008**, 2008, 1–8.
  13. Kneipp, J.; Kneipp, H.; Kneipp, K. *Chem. Soc. Rev.* **2008**, 37, 1052.
  14. Lee, S. J.; Guan, Z.; Xu, H.; Moskovits, M. *J. Phys. Chem. C* **2007**, 111, 17985.
  15. Banholzer, M. J.; Millstone, J. E.; Qin, L.; Mirkin, C. A. *Chem. Soc. Rev.* **2008**, 37, 885.
  16. Baker, G. A.; Moore, D. S. *Anal. Bioanal. Chem.* **2005**, 382, 1751.
  17. Herculano, R. D.; Silva, C. P.; Ereno, C.; Guimaraes, S. A. C.; Kinoshita, A.; Graeff, C. F. O. *Mater. Res.* **2009**, 12, 253.
  18. Ferreira, M.; Mendonça, R. J.; Coutinho-Netto, J.; Mulato, M. *Braz. J. Phys.* **2009**, 39, 564.
  19. Frade, M. A. C.; Cursi, I. B.; Andrade, F. F.; Coutinho-Netto, J.; Barbetta, F. M.; Foss, N. T. *Méd. Cutan. Iber. Lat. Am.* **2004**, 32, 157.
  20. Agostini, D. L. S.; Constantino, C. J. L.; Job, A. E. *J. Therm. Anal. Calorim.* **2008**, 91, 703.
  21. Cavalli, A.; Borissevitch, G.; Tabak, M.; Oliveira, O. N., Jr. *Thin Solid Films* **1996**, 284–285, 731.
  22. Jessel, N.; Atalar, F.; Lavalle, P.; Mutterer, J.; Decher, G.; Schaaf, P.; Voegel, J. C.; Ogier, J. *Adv. Mater.* **2003**, 15, 692.
  23. Ladam, G.; Schaaf, P.; Decher, G.; Voegel, J. C.; Cuinsinier, F. J. G. *Biomol. Eng.* **2002**, 19, 273.
  24. Goulet, P. J. G.; Dos Santos, D. S.; Alvarez-Puebla, R. A.; Oliveira, O. N., Jr.; Aroca, R. F. *Langmuir* **2005**, 21, 5576.
  25. Dos Santos, D. S.; Alvarez-Puebla, R. A.; Oliveira, O. N., Jr.; Aroca, R. F. *J. Mater. Chem.* **2005**, 15, 3045.
  26. Vaananen, D.; Ikonen, T.; Rokka, V. M.; Kuronen, P.; Serimaa, R.; Ollilainen, V. *J. Agric. Food Chem.* **2005**, 53, 5313.
  27. Barboza-Filho, C. G.; Cabrera, F. C.; Dos Santos, R. J.; De Saja Saez, J. A.; Job, A. E. *J. Exp. Parasitol.* **2012**, 130, 152.
  28. Grabar, K. C.; GrWith Freeman, R.; Hommer, M. B.; Natan, M. *J. Anal. Chem.* **1995**, 67, 735.
  29. Cabrera, F. C.; Aoki, P. H. B.; Aroca, R. F.; Constantino, C. J. L.; Dos Santos, D. S.; Job, A. E. *J. Raman Spectrosc.* **2012**, 43, 474, I. 4.
  30. De Jong, W. H.; Burger, M. C.; Verheijen, M. A.; Geertsma, R. E. *Materials* **2010**, 3, 4681.
  31. Sohn, B.-H.; Choi, J.-M.; Yoo, S. I.; Yun, S.-H.; Zin, W.-C.; Jung, J. C.; Kanehara, M.; Hirata, T.; Teranishi, T. *J. Am. Chem. Soc.* **2003**, 125, 6368.
  32. De Oliveira, L. C. S.; De Arruda, E. J.; Favaro, S. P.; Da Costa, R. B.; Gonçalves, P. S.; Job, A. E. *Thermochim. Acta* **2006**, 445, 27.
  33. Li, S.-D.; Yu, H.-P.; Zhu, C.-S.; Li, P.-S. *J. Appl. Polym. Sci.* **2000**, 75, 1339.
  34. Sicar, A. K. *Rubber Chem. Technol.* **1977**, 50, 71.
  35. Willian Callister, D., Jr. *Ciência e Engenharia de Materiais - Uma Introdução*, Editora LTC, **2002**, 5ª Edição, 327–332.